Inorg. Chem. **2007**, *46*, 8746–8751

Magnetic Properties of Bulk $BiCrO_3$ Studied with dc and ac Magnetization and Specific Heat

Alexei A. Belik,*,† Naohito Tsujii,‡ Hiroyuki Suzuki,‡ and Eiji Takayama-Muromachi†

Advanced Nano Materials Laboratory (ANML) and Quantum Beam Center, National Institute for Materials Science (NIMS), 1-1 Namiki, Tsukuba, Ibaraki 305-0044, Japan

Received June 5, 2007

Single-phased powder $BiCrO_3$ sample was prepared at 6 GPa and 1653 K. Its magnetic properties were investigated by dc/ac magnetization, magnetic relaxation, and specific heat measurements. Four anomalies of magnetic origin were found near 40, 75, 109, and 111 K. The long-range antiferromagnetic order with weak ferromagnetism occurs at $T_N = 109$ K. The ac susceptibilities showed that the transition near T_N is a two-step transition. Additional frequency-independent broad anomalies were observed on the real part of the ac susceptibilities near 75 K, likely, caused by the change in the magnetic easy axis. The dc magnetic susceptibilities also had anomalies at 75 K, and the isothermal magnetization curves and relaxation curves changed their behavior below 75 K. Below 40 K, frequency-dependent anomalies with very large temperature shifts were observed on both the real and imaginary parts of the ac susceptibilities. The monoclinic-to-orthorhombic structural phase transition near 420 K was investigated by magnetization and differential scanning calorimetry measurements.

1. Introduction

Multiferroic materials have received revival interest in recent years.[1−4] In multiferroic systems, two or all three of (anti)ferroelectricity, (anti)ferromagnetism, and ferroelasticity are observed in the same phase.[5] Such systems seem to be rare in nature, but they are quite interesting because of their possible applications in devices (e.g., multiple-state memory elements)[5] and new basic physics (e.g., ferroelectricity induced by charge ordering and spiral magnetic ordering).[6,7]

Bi-containing perovskites are promising candidates for multiferroic materials because of the presence of the stereochemically active lone electron pair of a Bi^{3+} ion. $BiMnO_3$ is a ferromagnet,[8−10] and $BiCrO_3$,[8,11] $BiFeO_3$,[12] $BiCoO_3$,[13] and $BiNiO_3$[14] are antiferromagnets with a weak ferromagnetic component in some cases resulting from spin canting. $BiFeO_3$ and $BiCoO_3$ definitely have polar structures, and the ferroelectric properties of $BiFeO_3$ were shown experimentally in a large number of works. $BiNiO_3$ crystallizes in the centrosymmetric space group $P\bar{1}$. $BiMnO_3$ was believed to adopt the noncentrosymmetric structure with space group $C2$,[9,15] and one paper reported its ferroelectric properties.[16] Thin film $BiMnO_3$ samples showed large second harmonic generation especially under applied electric field.[17] However, it was shown recently that the crystal structure of bulk $BiMnO_3$ can be very well described by the centrosymmetric model

* To whom correspondence should be addressed. E-mail: Alexei.BELIK@nims.go.jp.
† ANML, NIMS.
‡ Quantum Beam Center, NIMS.

(1) Eerenstein, W.; Mathur, N. D.; Scott, J. F. *Nature* **2006**, *442*, 759.
(2) Ramesh, R.; Spaldin, N. A. *Nat. Mater.* **2007**, *6*, 21.
(3) Cheong, S.-W.; Mostovoy, M. *Nat. Mater.* **2007**, *6*, 13.
(4) Fiebig, M. *J. Phys. D: Appl. Phys.* **2005**, *38*, R123.
(5) Hill, N. A. *J. Phys. Chem. B* **2000**, *104*, 6694.
(6) Ikeda, N.; Ohsumi, H.; Ohwada, K.; Ishii, K.; Inami, T.; Kakurai, K.; Murakami, Y.; Yoshii, K.; Mori, S.; Horibe, Y.; Kito, H. *Nature* **2005**, *436*, 1136.
(7) Kimura, T.; Goto, T.; Shintani, H.; Ishizaka, K.; Arima, T.; Tokura, Y. *Nature* **2003**, *426*, 55.
(8) Sugawara, F.; Iiida, S.; Syono, Y.; Akimoto, S. *J. Phys. Soc. Jpn.* **1968**, *25*, 1553.
(9) Moreira dos Santos, A.; Cheetham, A. K.; Atou, T.; Syono, Y.; Yamaguchi, Y.; Ohoyama, K.; Chiba, H.; Rao, C. N. R. *Phys. Rev. B* **2002**, *66*, 064425.
(10) Kimura, T.; Kawamoto, S.; Yamada, I.; Azuma, M.; Takano, M.; Tokura, Y. *Phys. Rev. B* **2003**, *67*, 180401(R).
(11) Niitaka, S.; Azuma, M.; Takano, M.; Nishibori, E.; Takata, M.; Sakata, M. *Solid State Ionics* **2004**, *172*, 557.
(12) Wang, J.; Neaton, J. B.; Zheng, H.; Nagarajan, V.; Ogale, S. B.; Liu, B.; Viehland, D.; Vaithyanathan, V.; Schlom, D. G.; Waghmare, U. V.; Spaldin, N. A.; Rabe, K. M.; Wuttig, M.; Ramesh, R. *Science* **2003**, *299*, 1719.
(13) Belik, A. A.; Iikubo, S.; Kodama, K.; Igawa, N.; Shamoto, S.; Niitaka, S.; Azuma, M.; Shimakawa, Y.; Takano, M.; Izumi, F.; Takayama-Muromachi, E. *Chem. Mater.* **2006**, *18*, 798.
(14) Ishiwata, S.; Azuma, M.; Takano, M.; Nishibori, E.; Takata, M.; Sakata, M.; Kato, K. *J. Mater. Chem.* **2002**, *12*, 3733.
(15) Atou, T.; Chiba, H.; Ohoyama, K.; Yamaguchi, Y.; Syono, Y. *J. Solid State Chem.* **1999**, *145*, 639.

10.1021/ic701099f CCC: $37.00
Published on Web 09/14/2007

with space group $C2/c$.[18,19] In the case of $BiCrO_3$, which was reported to have the same structure as $BiMnO_3$,[11] antiferroelectric properties were demonstrated experimentally in thin film samples[20a] in agreement with the theoretical studies,[21] and ferroelectricity was caused by an applied electric field.[20a] Antiferroelectric properties of $BiCrO_3$ suggest that it has a centrosymmetric crystal structure. $BiCrO_3$ demonstrates a structural phase transition from the monoclinic phase to the $GdFeO_3$-type orthorhombic phase near 410−420 K.[8,11] Magnetic properties of bulk $BiCrO_3$ have been investigated quite poorly. It was reported that an antiferromagnetic transition with a weak spontaneous moment appeared below 123 or 114 K.[8,11] The weak spontaneous moment increased rapidly below 95 K with deference between the zero-field-cooled and field-cooled magnetization curves below 75 K.[8,11] The magnetic phase-transition temperatures are considerably shifted in thin film $BiCrO_3$ samples.[20]

To achieve a better understanding of the properties of $BiCrO_3$, we have performed dc/ac magnetization, magnetic relaxation, and specific heat measurements on single-phase powder samples. These measurements revealed four anomalies of magnetic origin, the existence of frequency-dependent anomalies with very large temperature shifts below 40 K, and a two-step antiferromagnetic transition near 109 K.

2. Experimental Section

A mixture of Bi_2O_3 (99.99%) and Cr_2O_3 (99.9%) with an amount-of-substance ratio of 1:1 was placed in Au capsules and treated at 6 GPa in a belt-type high-pressure apparatus at 1653 K for 60−70 min (heating rate 140 K min^{-1}). After heat treatment, the samples were quenched to room temperature (RT), and the pressure was slowly released. The resultant samples were khaki-green dense pellets. X-ray powder diffraction (XRD) showed that the samples were single phase (see Supporting Information). The lattice parameters were determined by the Rietveld method with the $C2/c$ model[18] using RIETAN-2000.[22] The refined lattice parameters (a = 9.4684(3) Å, b = 5.4838(2) Å, c = 9.5932(3) Å, and β = 108.571(3)°) and XRD pattern are in good agreement with the previously reported lattice parameters and XRD pattern.[11] Note that at lower synthesis temperatures (1370−1600 K), the samples contained impurities of Bi_2O_3 (the high-pressure modification)[23] and Cr_2O_3. Our synthesis conditions (especially temperature) were different compared with the previously reported ones (3.5−5.5 GPa and 973−1073 K[8] and 4 GPa and 993 K).[11]

(16) dos Santos, A. M.; Parashar, S.; Raju, A. R.; Zhao, Y. S.; Cheetham, A. K.; Rao, C. N. R. *Solid State Commun.* **2002**, *122*, 49.
(17) Sharan, A.; Lettieri, J.; Jia, Y.; Tian, W.; Pan, X.; Schlom, D. G.; Gopalan, V. *Phys. Rev. B* **2004**, *69*, 214109.
(18) Belik, A. A.; Iikubo, S.; Yokosawa, T.; Kodama, K.; Igawa, N.; Shamoto, S.; Azuma, M.; Takano, M.; Kimoto, K.; Matsui, Y.; Takayama-Muromachi, E. *J. Am. Chem. Soc.* **2007**, *129*, 971.
(19) Montanari, E.; Calestani, G.; Righi, L.; Gilioli, E.; Bolzoni, F.; Knight, K. S.; Radaelli, P. G. *Phys. Rev. B* **2007**, *75*, 220101(R).
(20) (a) Kim, D. H.; Lee, H. N.; Varela, M.; Christen, H. M. *Appl. Phys. Lett.* **2006**, *89*, 162904. (b) Murakami, M.; Fujino, S.; Lim, S. H.; Long, C. J.; Salamanca-Riba, L. G.; Wuttig, M.; Takeuchi, I.; Nagarajan, V.; Varatharajan, A. *Appl. Phys. Lett.* **2006**, *88*, 152902. (c) Geprags, S.; Opel, M.; Goennenwein, S. T. B.; Gross, R. *Philos. Mag. Lett.* **2007**, *87*, 141.
(21) (a) Hill, N. A.; Battig, P.; Daul, C. *J. Phys. Chem. B* **2002**, *106*, 3383. (b) Baettig, P.; Ederer, C.; Spaldin, N. A. *Phys. Rev. B* **2005**, *72*, 214105.
(22) Izumi, F.; Ikeda, T. *Mater. Sci. Forum* **2000**, *321−324*, 198.
(23) Atou, T.; Faqir, H.; Kikuchi, M.; Chiba, H.; Syono, Y. *Mater. Res. Bull.* **1998**, *33*, 289.

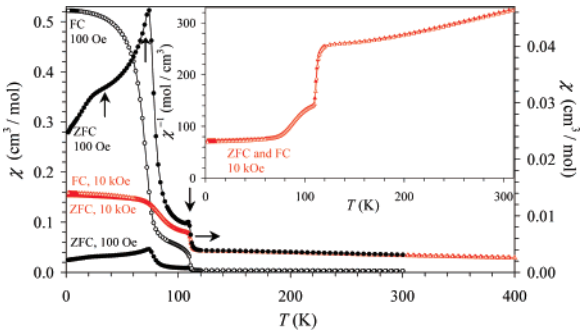

Figure 1. ZFC and FC dc magnetic susceptibility ($\chi = \mathbf{M}/\mathbf{H}$) curves of $BiCrO_3$ measured at 100 Oe (the left-hand axis) and 10 kOe (the right-hand axis). The ZFC curve at 100 Oe is also plotted using the right-hand axis for the clarity. Inset shows the inverse ZFC and FC curves at 10 kOe. The vertical arrows give the positions of the anomalies.

Magnetic susceptibilities, $\chi = \mathbf{M}/\mathbf{H}$, of $BiCrO_3$ were measured on a SQUID magnetometer (Quantum Design, MPMS) between 2 and 400 K in applied fields of 100 Oe and 10 kOe and between 300 and 600 K in an applied field of 50 kOe using a furnace under both zero-field-cooled (ZFC) and field-cooled (FC) conditions. Isothermal magnetization measurements were performed between −10 kOe and 10 kOe at 5, 60, 90, and 130 K. Isothermal magnetization curves were also taken at 1.8 K between 0 and 300 kOe using a hybrid magnet of NIMS. Frequency-dependent ac susceptibility measurements of $BiCrO_3$ at zero static magnetic field were performed with a Quantum Design MPMS instrument from 200 to 2 K at frequencies (f) of 1.99, 9.99, 20, 99.9, 498.7, and 997.3 Hz and an applied oscillating magnetic field (H_{ac}) of 5 Oe. We also measured the ac susceptibilities of $BiCrO_3$ at zero static magnetic field and frequency of 99.9 Hz at different H_{ac} (0.5, 2, and 5 Oe; the maximum H_{ac} of our instrument is 5 Oe) and at H_{ac} = 5 Oe, f = 1.99 and 498.7 Hz, and different static magnetic fields H_{dc} (0.1, 0.5, 1, 3, and 10 kOe). The time-dependent relaxation curves were measured at 100 Oe after the sample was cooled from 200 K to the desired temperature at zero magnetic field (the waiting time before setting 100 Oe was 5 min). The relaxation curves were measured several times at each temperature to check the reproducibility. Good agreement between different measurements was observed (see Supporting Information). Another protocol for the relaxation measurements, namely, cooling in a magnetic field and measuring in zero magnetic field, was not used because there is always a small trapped magnetic field inside the superconducting magnet. This trapped field has strong effect and considerably reduces reproducibility. The specific heat, C_p, of $BiCrO_3$ at 0 and 90 kOe was recorded between 2 and 300 K upon cooling by a pulse relaxation method using a commercial calorimeter (Quantum Design PPMS).

Differential scanning calorimetry (DSC) curves of $BiCrO_3$ were recorded on a SII Exstar 6000 (DSC 6220) system at a heating/cooling rate of 10 K min^{-1} from 133 to 873 K in semiclosed aluminum capsules. The DSC runs were cycled between 300 and 520 K several times; then the samples were heated up to 873 K, and finally the DSC runs were cycled again between 300 and 470 K.

3. Results and Discussion

Figure 1 shows magnetic susceptibilities of $BiCrO_3$ between 2 and 400 K. Three anomalies are seen from the ZFC χ versus T curve measured at 100 Oe: anomalies near T_1 = 40 K, T_2 = 74 K, and T_N = 109 K. The difference between the ZFC and FC curves is clearly seen below 109

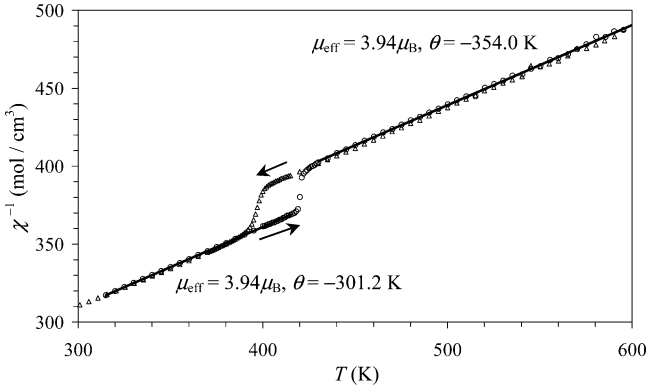

Figure 2. Inverse magnetic susceptibility curves measured at 50 kOe between 300 and 600 K (symbols) with the Curie−Weiss fits (lines). The parameters, μ_{eff} and θ, of the fits are given.

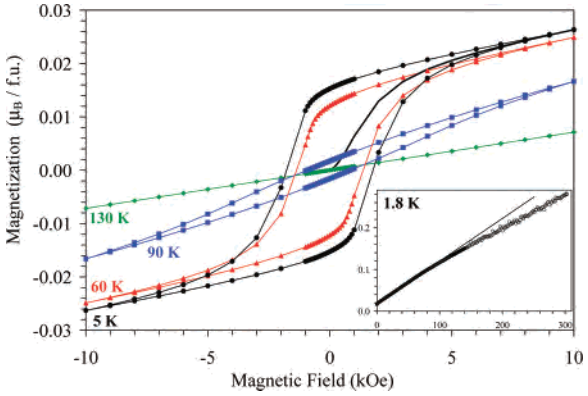

Figure 3. Isothermal magnetization curves at 5, 60, 90, and 130 K between −10 and 10 kOe. Inset shows the isothermal magnetization curve measured at 1.8 K from 300 kOe to 0 kOe (symbols); the line is obtained by fitting between 0 and 80 kOe and emphasizes the curvature near 100 kOe. The axes units are the same as those in the main figure.

K. There is a weak ferromagnetic response below 109 K. The weak spontaneous moment and the difference between the ZFC and FC curves increase rapidly below T_2, in agreement with the previous works.[8,11] The ZFC and FC curves almost coincide with each other when measured at 10 kOe. No anomalies were detected near 40 K on the ZFC and FC curves at 10 kOe, but the anomalies near 74 and 109 K are detectable. The χ^{-1} versus T curves below 300 K in the paramagnetic state showed noticeable deviation from the Curie−Weiss law (especially below 200 K where the χ^{-1} vs T curves have a tendency to plateau). This behavior is reminiscent of the presence of short-range correlation and the origin of the anomalously large effective magnetic moment reported in the literature ($4.7\mu_B$ for the low-temperature monoclinic phase).[8] The high-temperature regions (315−415 and 430−600 K, Figure 2) are fit by the Curie−Weiss equation

$$\chi^{-1}(T) = 3k_B(T - \theta)/(\mu^2_{eff}N) \quad (1)$$

where μ_{eff} is effective magnetic moment, N is Avogadro's number, k_B is Boltzmann's constant, and θ is the Weiss constant. The fitted parameters are given in Figure 2. The observed jumps at 420 (upon heating) and 400 K (upon cooling) are caused by the structural monoclinic-to-orthorhombic phase transition. The phase transition temperature is in good agreement with the previous data (410 K[8] and between 420 and 440 K).[11] The effective magnetic moment ($3.94\mu_B$) is the same at 315−415 K (the monoclinic phase) and 430−600 K (the orthorhombic phase) and close to the localized Cr^{3+} moment of $3.87\mu_B$. The absolute value of the Weiss constant increased at 430−600 K, probably reflecting the change of the Cr−O−Cr bond angles that become more close to 180° in the high-temperature orthorhombic phase.

Figure 3 depicts the isothermal magnetization curves. Almost no hysteresis is observed at 130 K (the remnant magnetization (M_r) was about $2 \times 10^{-5}\mu_B$ per a Cr^{3+} ion). A noticeable hysteresis is seen below T_N (at 90 K). The hysteresis changes its form below T_2 (at 60 K), and the form remains the same at lower temperatures (at 5 K). The M versus H data confirm that intrinsic changes occur in the sample below T_2. Even the weak ferromagnetic moment appears below T_N, the clear ferromagnetic hysteresis loop (that is, having squarelike form) is developed only below T_2. High-field magnetization measurements at 1.8 K (inset of Figure 3) show a small curvature of the M versus H curve above 100 kOe, while between 0 and 80 kOe, a linear behavior is observed.

The magnetic structure of $BiCrO_3$ is not known now. However, $BiCrO_3$ should have the G-type antiferromagnetic structure as assumed in ref 8 and predicted in ref 21a. There should be two crystallographic Cr sites (4e and 4d) in the monoclinic modification of $BiCrO_3$ by analogy with $BiMnO_3$.[18] Therefore, the simple G-type antiferromagnetic structure can be realized with the propagation vector $k = [0,0,0]$ and magnetic moments along the b-axis (similar to the direction of magnetic moments in $BiMnO_3$).[9,19] The symmetry allows spin canting at the 4d site along the b direction and, therefore, the appearance of weak ferromagnetism.

Figure 4 gives the ac susceptibility curves of $BiCrO_3$ at $H_{dc} = 0$ Oe. The χ'' versus T curves clearly show that the transition near $T_N = 109$ K is a two-step transition with sharp peaks on the χ'' versus T curves at $T_{N1} = 108.5$ and $T_{N2} = 111.0$ K. The peaks on both χ' versus T and χ'' versus T curves signal the appearance of a weak ferromagnetic component. Broad anomalies appear on both χ' versus T and χ'' versus T curves near $T_2 = 74$ K. The χ' versus T curves are frequency-independent, while there is suppression of anomalies with increasing frequency (without the temperature shifts) on the χ'' versus T curves. Strong frequency-dependent anomalies are observed below $T_1 = 40$ K, especially the temperature shifts of the χ'' versus T curves are pronounced (the maximum is observed at $T_m = 12$ K for $f = 1.99$ Hz and at $T_m = 31$ K for $f = 997.3$ Hz). A criterion that can be used to distinguish the freezinglike processes is the frequency dependence of T_m: $\delta T_m = \Delta T_m/(T_m \Delta \log f)$. With the above T_m values, we obtain $\delta T_m = 0.23$. The shifts of the χ'' versus T curves are too large for typical spin glasses ($\delta T_m = 0.005$−0.06) but are typical for superparamagnets ($\delta T_m = 0.3$).[24] To analyze the frequency shift of T_m, three approaches are

(24) Mydosh, J. A. *Spin Glasses: An Experimental Introduction*; Taylor & Francis: London, 1993.

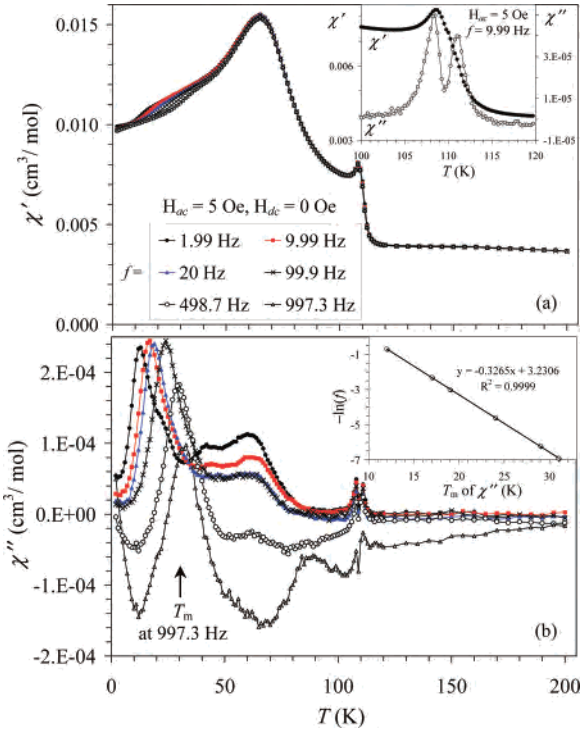

Figure 4. The real χ' (a) and imaginary χ'' (b) parts of the ac susceptibility of $BiCrO_3$ as a function of temperature at different frequencies, $f = 1.99$, 9.99, 20, 99.9 498.7, and 997.3 Hz. Measurements were performed upon cooling at zero static field using an ac field with the amplitude $H_{ac} = 5$ Oe. The inset in panel a shows the detailed measurements of the χ' vs T and χ'' vs T curves at $f = 9.99$ Hz in the vicinity of T_N. The inset in panel b shows the ln(1/f) vs T_m curve, where T_m is the position of the maximum on the χ'' vs T curves at the given f.

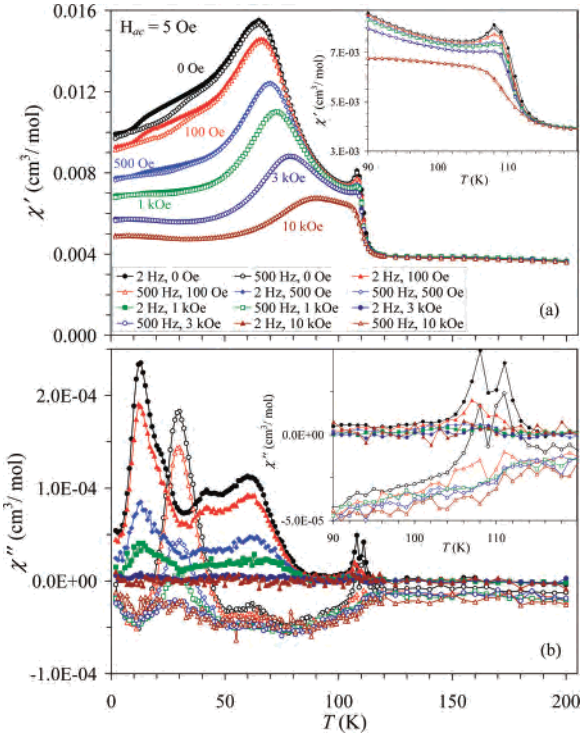

Figure 5. Real χ' (a) and imaginary χ'' (b) parts of the ac susceptibility of $BiCrO_3$ as a function of temperature at frequencies of 1.99 Hz (full symbols) and 498.7 Hz (white symbols) and different static magnetic fields $H_{dc} = 0.1$, 0.5, 1, 3, and 10 kOe. Measurements were performed upon cooling for each H_{dc} with $H_{ac} = 5$ Oe. The insets show the details near T_N.

usually considered: (1) the thermal activated (Arrhenius) law $f = f_0 \exp[-E_a/(k_B T_m)]$ for isolated particles, (2) the Vogel−Fulcher law $f = f_0 \exp[-E_a/(k_B(T_m - T_0))]$ for particles with interaction, and (3) the dynamic scaling theory.[25] The ln f versus $1/T_m$ plot shows a noticeable deviation from the linear behavior (see Supporting Information). The $1/\ln(f_0/f)$ versus T_m plot with $f_0 = 10^{12}$ Hz is close to linear, but the physically unrealistic values are obtained from the fit $E_a/k_B = 1700$ K and $T_0 = -50$ K. Attempts to apply the dynamic scaling theory failed. Actually there is a very good linear relation between ln f and T_m (the inset of Figure 4b). Therefore, additional experiments will be needed to understand the origin of these "superparamagnetic-like" anomalies. We note here that the superparamagnetic-like anomalies in magnetic properties are often explained by a phase separation and the formation of ferromagnetic nanoclusters in stoichiometric single-phase samples, for example, $BaCoO_3$[26] and $RuSr_2GdCu_2O_8$,[27] or by structural disorder, for example, Ca_3CoRhO_6.[28]

No difference is found for the χ' versus T and χ'' versus T curves measured at H_{ac} between 0.5 and 5 Oe. At $H_{ac} = 0.5$ Oe, the data were too noisy, even though the sample weight was 0.67 g. The covered range of H_{ac} is rather small. Nevertheless, the absence of any dependence of χ' and χ'' on H_{ac} usually indicates that the anomalies are intrinsic to the sample and not related to the domain wall movements.

The effect of static magnetic field H_{dc} is illustrated in Figure 5. Almost no frequency dependence is observed near T_1 at $H_{dc} \geq 3$ kOe, and anomalies on the χ'' vs T curves are also almost suppressed. The double anomalies near T_N on the χ'' vs T curves are suppressed at $H_{dc} \geq 500$ Oe. This result may show that the magnetic field removes spin canting and stabilizes the antiferromagnetic state. The broad peak near T_2 is shifted to higher temperatures with increasing H_{dc}. This fact may indicate that the magnetic state below T_2 is stabilized by magnetic field. The H_{dc} has no effect on the peak positions of χ'' below T_1 (that is, T_m); only the intensity of the χ'' peaks at T_m is suppressed. Note that the similar effect of H_{dc} on the superparamagnetic-like anomalies was observed in Ca_3CoRhO_6.[28]

Note that we have investigated several $BiCrO_3$ samples prepared using slightly different conditions (varying temperature between 1600 and 1770 K). All the samples showed four magnetic anomalies described above. The temperature positions of the χ' and χ'' anomalies near T_1 and T_N were almost independent of the sample. However, the temperature positions of the anomalies near T_2 were slightly sample-dependent (see Supporting Information).

We have also probed the magnetic relaxation behavior in different temperature ranges (Figure 6). The relaxation was observed at 10 K and reached maximum at $T_1 = 40$ K below which the frequency dependence on χ' versus T and χ'' versus

(25) Mukherjee, S.; Pal, A. K.; Bhattacharya, S.; Raittila, J. *Phys. Rev. B* **2006**, *74*, 104413.
(26) Botta, P. M.; Pardo, V.; Baldomir, D.; de la Calle, C.; Alonso, J. A.; Rivas, J. *Phys. Rev. B* **2006**, *74*, 214415.
(27) Cimberle, M. R.; Masini, R.; Canepa, F.; Costa, G.; Vecchione, A.; Polichetti, M.; Ciancio, R. *Phys. Rev. B* **2006**, *73*, 214424.
(28) Sampathkumaran, E. V.; Niazi, A. *Phys. Rev. B* **2002**, *65*, 180401.

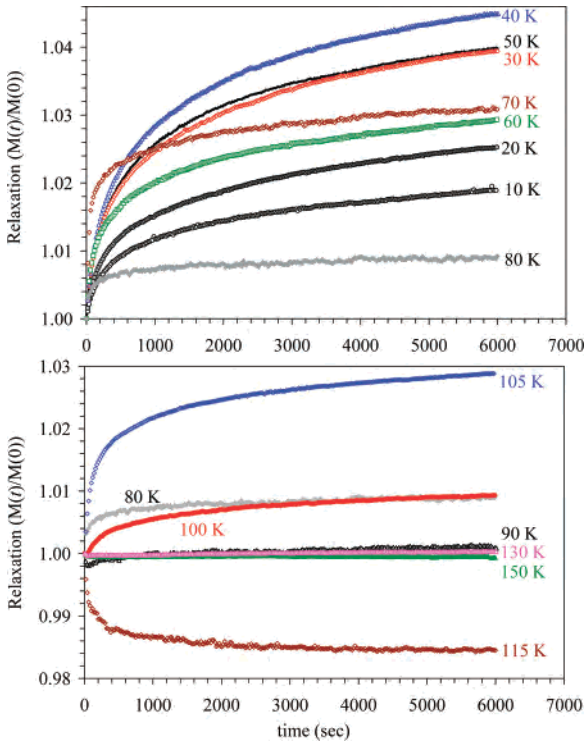

Figure 6. Relative change of magnetization M(*t*)/M(0) as a function of time (relaxation). The curves were measured at 100 Oe after the sample was cooled from 200 K to the desired temperature at zero magnetic field.

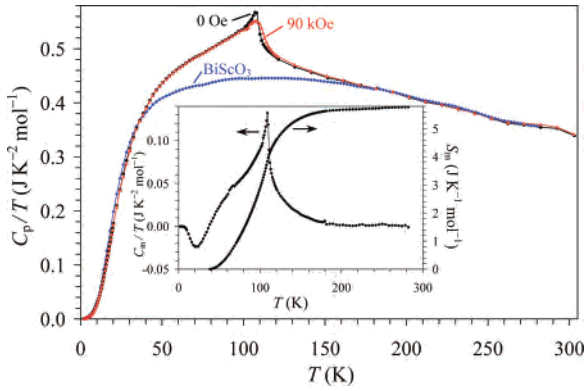

Figure 7. C_p/T vs T curves between 2 and 300 K for $BiCrO_3$ (at 0 and 90 kOe) and $BiScO_3$. Inset shows the C_m/T vs T and S_m vs T curves for $BiCrO_3$. The magnetic specific heat (C_m) was obtained by subtraction of the total specific heat of $BiScO_3$ from that of $BiCrO_3$. S_m is the magnetic entropy.

T curves started. Then the relaxation rate decreases with increasing temperature between T_1 and T_2. Above about T_2, the relaxation changes its behavior, that is, the relaxation is much faster in the first minutes and then proceeds much more slowly. With increasing temperature, the relaxation rate reaches minimum at 90 K and starts to increase when approaching T_N. Note that at 90 and 100 K, the magnetization first decreases during the first seconds and then starts to increase (see also Supporting Information). Just above T_N at 115 K, the relaxation was negative, that is, the magnetic moment decreased with time in an applied magnetic field. Well above T_N at 130 and 150 K, almost no relaxation was found.

Figure 7 shows the specific heat of $BiCrO_3$ plotted as C_p/T versus T. The λ-type anomaly on the C_p versus T is observed with the maximum at $T_N = 109$ K. However, no anomalies are found near T_1 and T_2. This fact may indicate that the global antiferromagnetic structure does not change below T_N; only magnetic easy axis or canting angle is changed. The lattice contribution (C_l) in $BiCrO_3$ is estimated using $BiScO_3$ containing no magnetic ions.[29] In the temperature ranges of 2−38 and 180−300 K, the C_p versus T curves of $BiCrO_3$ and $BiScO_3$ are very similar to each other indicating that $BiScO_3$ can give good approximation to the C_l. The magnetic specific heat (C_m) of $BiCrO_3$ is obtained by subtraction of the total specific heat of $BiScO_3$ from that of $BiCrO_3$. Between 6 and 38 K, the specific heat of $BiScO_3$ was a little bit larger than that of $BiCrO_3$. Therefore, to calculate the magnetic entropy, we assumed that $C_m(BiCrO_3) = 0$ between 2 and 38 K. The magnetic entropy was obtained using the equation

$$S_m = \int (C_m/T)\mathrm{d}T \qquad (2)$$

S_m is 5.77 J K^{-1} mol^{-1}, which is much smaller than the spin-only value of $R \ln(2S+1) = R \ln 4 = 11.5$ J K^{-1} mol^{-1} expected for the $S = 3/2$ systems (S is spin). Note that in the case of $BiMnO_3$, the magnetic entropy estimated in the same way was noticeably larger than the spin-only value.[30] Because $BiScO_3$ gives a rather good approximation to the C_l, the strongly reduced S_m cannot be simply explained by difficulties in the estimation of the C_l. Surprisingly, the experimental S_m value of $BiCrO_3$ is very close to that of an $S = 1/2$ system (5.76 J K^{-1} mol^{-1}). It could be accidental. Nevertheless, in this context, we note that a Co^{2+} ion with a spin of 3/2 is often described as having an effective spin of 1/2 at low temperatures because of effects of the crystal field and strong single-ion anisotropy,[31] and magnetic entropy of Co^{2+} approached 5.76 J K^{-1} mol^{-1} at low temperatures. About 67% of the entropy in $BiCrO_3$ is gained below T_N. The rest of the entropy gained between T_N and 180 K may be attributed to the short-range correlations in agreement with the large deviation of the χ^{-1} versus T curves from the Curie−Weiss behavior in the paramagnetic state. The magnetic field has a very weak effect on the specific heat of $BiCrO_3$ as expected for an antiferromagnetic system with large T_N (only small smearing of the transition was observed near T_N). In the case of ferromagnetic $BiMnO_3$, the magnetic field had a strong effect on the specific heat.[30]

The structural phase transition in $BiCrO_3$ is accompanied by noticeable anomalies on magnetic susceptibilities (Figure 2).[8] This phase transition and the thermal stability of $BiCrO_3$ are investigated in more details by the DSC measurements (Figure 8). The cycling of the DSC curves below 520 K gave very reproducible results. However, after $BiCrO_3$ was heated to 873 K, the phase-transition temperature decreases from 416 K (the position of the DSC maximum on heating) to 386 K. The XRD data collected after heating up to 873 K showed the appearance of a very weak reflection from

(29) Belik, A. A.; Iikubo, S.; Kodama, K.; Igawa, N.; Shamoto, S.; Maie, M.; Nagai, T.; Matsui, Y.; Stefanovich, S. Yu.; Lazoryak, B. I.; Takayama-Muromachi, E. *J. Am. Chem. Soc.* **2006**, *128*, 706.
(30) Belik, A. A.; Takayama-Muromachi, E. *Inorg. Chem.* **2006**, *45*, 10224.
(31) de Jongh, L. J.; Miedema, A. R. *Adv. Phys.* **2001**, *50*, 947.

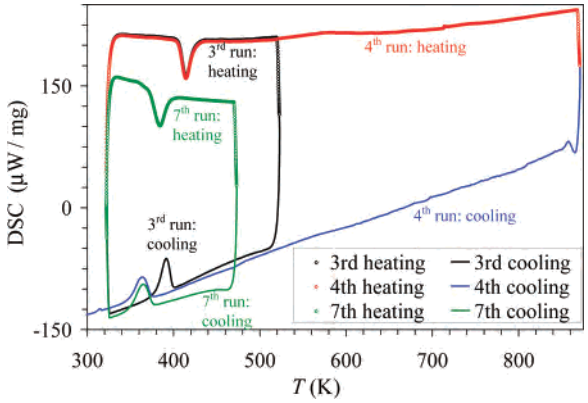

Figure 8. DSC curves of $BiCrO_3$. The first (not shown), second (not shown), and third cycles are between 320 and 520 K. During the forth cycle, the $BiCrO_3$ sample is heated up to 873 K. The fifth (not shown), sixth (not shown), and seventh cycles are between 320 and 470 K. There was no difference between the fifth, sixth, and seventh cycles. However, note the difference between the third and seventh cycles.

$Bi_{25}CrO_{39}$ (see Supporting Information), in addition to the main phase of $BiCrO_3$. This result indicates that the shift of the phase transition temperature by 30 K can be explained by the partial sample decomposition or by oxygen content changes. No anomalies corresponding to the decomposition process were found on the DSC curves indicating that the decomposition proceeds very slowly. It seems that there is strong effect of the stoichiometry of $BiCrO_3$ on the phase-transition temperatures. In the previous works on the bulk $BiCrO_3$, the samples contained some impurities.[8,11] The stoichiometry effect can explain the difference in T_N (109 K in our work, 114 K in ref 11, and 123 K in ref 8).

In conclusion, the obtained results revealed that $BiCrO_3$ demonstrates interesting magnetic properties at low temperatures including the two-step antiferromagnetic transition, the frequency-dependent anomalies with large temperature shifts, and large contribution of short-range correlations. Neutron diffraction and electron microscopy observations at low temperatures are desirable for further investigation of $BiCrO_3$. We hope that this work will motivate additional investigations of this poorly studied (compared with $BiMnO_3$) compound.

Supporting Information Available: XRD patterns of the as-prepared $BiCrO_3$ and after the DSC experiment up to 873 K (Figure S1), the analyses of the frequency shift of T_m (Figure S2), reproducibility of the relaxation curves (Figure S3), the dc/ac magnetic susceptibility curves for different $BiCrO_3$ samples (Figure S4), and the ac susceptibilities at different H_{ac} (Figure S5) (PDF). This material is available free of charge via the Internet at http://pubs.acs.org.

IC701099F